BLAST LOADING COMPUTATIONS OVER COMPLEX STRUCTURES

Andrew Mark
U.S. Army Ballistic Research Laboratory
U.S. Army Armament Research and Development Command
Aberdeen Proving Ground, Maryland 21005

and

Paul Kutler
Applied Computational Aerodynamics Branch
NASA Ames Research Center
Moffett Field, California 94035

ABSTRACT

Computational results of shock waves impinging on a truck-like target and the ensuing diffraction flowfield are presented. The Euler equations are solved with MacCormack's explicit finite difference scheme. Computed pressures on the surface of the model compare favorably with experimental results from shock tube experiments. Isopycnics for the diffraction phase are also presented and show the time-dependent development of vortices generated at the various corners of the model.

I. INTRODUCTION

The accurate prediction of the effects of blast waves impinging on vehicles and structures is essential in the design, survivability, and hence effectiveness of these configurations. The problem is stated pictorially in Figure 1. Detailed experimental blast wave interaction data is both costly and difficult to obtain. Moreover, these experiments frequently do not provide a complete picture of the blast wave interaction flowfield. Actual experiments, in fact, only yield pressure data at a few selected points on the models. As a consequence essential design parameters are often difficult to define.

An alternative to the experimental description of the blast wave interaction phenomenon is the use of computational fluid dynamics. This is the approach adopted here. Accurate finite difference simulations offer the possibility of providing design data at a relatively low cost. Such a simulation provides a complete flowfield description that is essential to a fundamental understanding of the fluid mechanics and a necessity for an effective structural design. The numerically generated flowfield data can then be integrated to yield other vital information such as the total loads, center of pressure, and overturning moments.

In the present paper, these "shock-capturing" flowfield simulation techniques have been adapted to the blast wave/target interaction problem for a configuration of a military truck-like shape carrying a communications shelter. For two-dimensional simplicity, the wheels, canvas canopy and windshield have been omitted. Computational results are compared with experimental data from a shock tube.

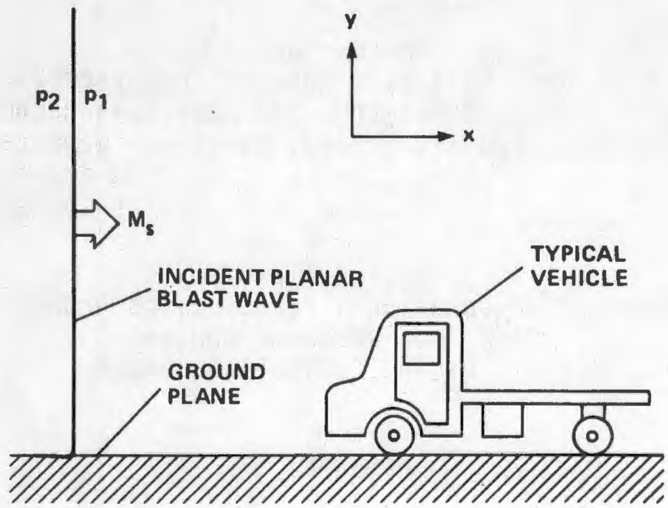

Figure 1. Blast wave-vehicle interaction problem.

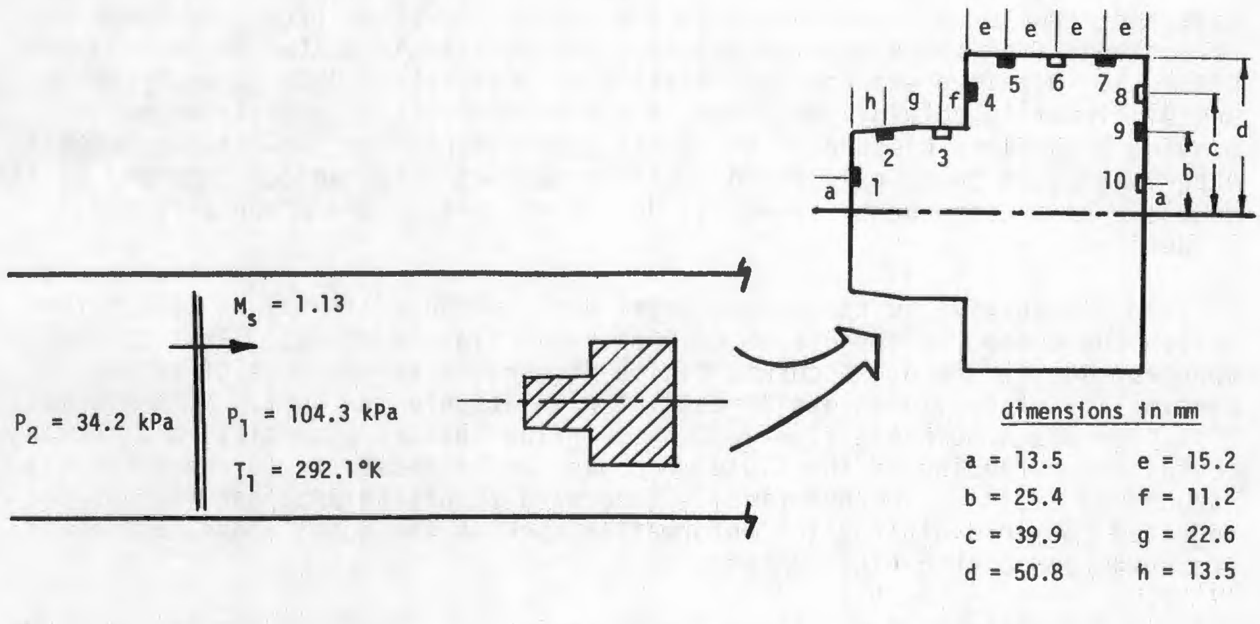

Figure 2. Shock tube experimental conditions for shock wave/truck interaction.

II. THEORETICAL CONSIDERATIONS

Several assumptions are made in the present study of blast wave encounters with targets. The first is that the blast wave is assumed to be planar relative to the target and that conditions behind the wave can be adequately and consistently described. Secondly, viscous effects are ignored. Finally, any effects which result from radiative heating on the target are assumed negligible, and a perfect gas equation of state is employed.

Under the above assumptions, the governing partial differential equations are the unsteady Euler equations which were solved by MacCormack's explicit finite-difference procedure with an additional fourth-order dissipation term (1). This method is a second-order, noncentered predictor-corrector scheme and appears as follows:

$$\begin{aligned} \bar{q} &= q^n - \Delta t(\Delta_\xi E^n + \Delta_\eta F^n) \\ q^{n+1} &= \frac{1}{2}\left[\bar{q} + q^n - \Delta t(\nabla_\xi \bar{E} + \nabla_\eta \bar{F}) + \varepsilon D^n\right] \end{aligned} \qquad (1)$$

where $\bar{E}$ implies that the flux vector E is evaluated using elements of the predicted value $\bar{q}$, and Δ and ∇ are the standard forward and backward difference operators. The quantity D represents a fourth-order dissipation term in both directions whose effect is governed by the dissipation constant ε.

III. RESULTS AND DISCUSSION

The physical and computational truck model that was used had no canvas top (cab) or windshield. These are light target components, easily destroyed by small overpressures, and represent an insignificant obstruction to the blast loading. In addition, the wheels were omitted from the model to permit a two-dimensional representation. The overall shape is meant to represent a 2½ ton truck carrying a communications shelter. A physical description of the model with its transducer positions is shown on the right side of Figure 2. This figure also shows a schematic of the test setup used in the shock tube. The model was built with identical mirror halves which were installed in the center of the shock tube, halfway between floor and ceiling. This type of installation avoids the viscous effects behind the shock on a floor mounted model. The Euler equations in the computations more closely approximate this condition. The midplane (or mirror plane) is treated like a symmetry boundary in the computations.

Figure 3 shows comparisons of pressure-time histories between the computations and the experiment. The "noisier" curves in these figures are the experimental results obtained at the Ballistic Research Laboratory by Bulmash (2). Six of the stations around the model are compared. These are indicated by the black dot in each inset figure. The computation was performed assuming free field conditions (no tube wall), so that wall reflections appearing in the experiment are not present in the computations. These occur at approximately 1.5 and 3 ms in Figure 3a. The same waves show up at different times in successive figures, which depend to some extent on the changing flow conditions, but more importantly, on the proximity of the affected surfaces (transducers) to the tube wall.

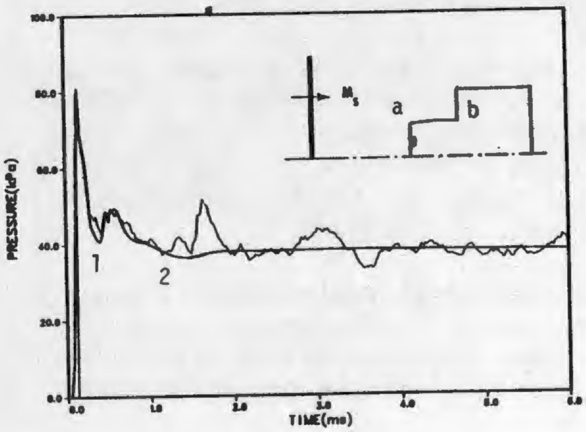

(a) gage location 1

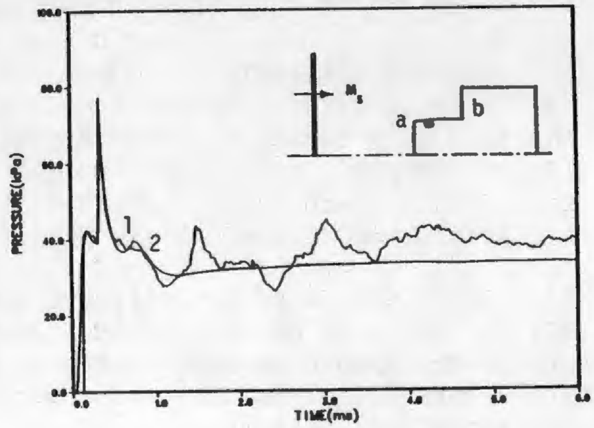

(b) gage location 2

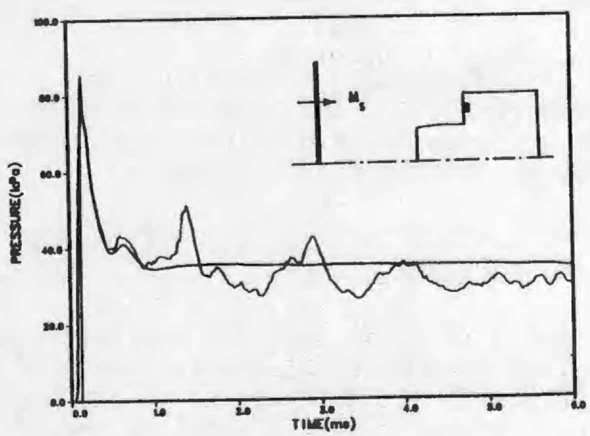

(c) gage location 4

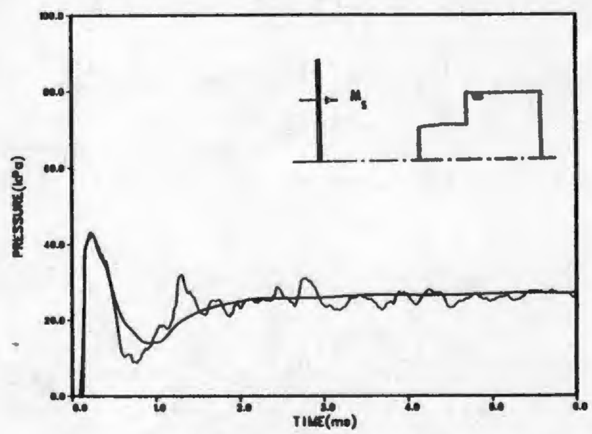

(d) gage location 5

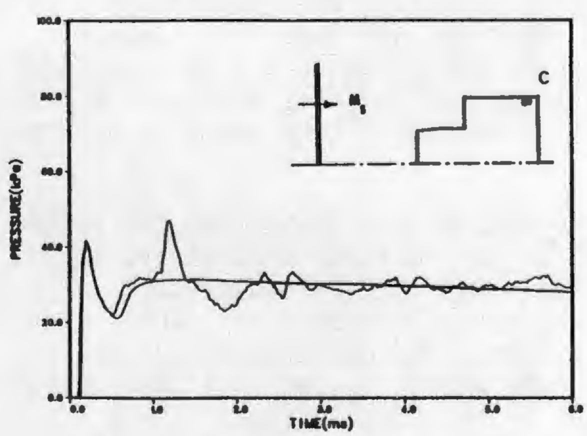

(e) gage location 7

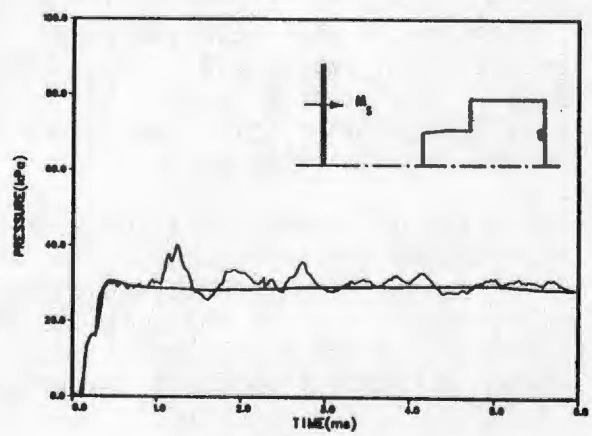

(f) gage location 9

Figure 3. Pressure-time history for blast wave/truck interaction. (Shock strength overpressure = 34.2 kPa)

Much detail is evidenced in the results if one examines the curves closely. As an example, the pressure rise for the early part of Figure 3a is caused by the flow stagnating in front of the truck and the decay is caused by the rarefaction wave generated at corner a and sweeping down the front of the "grill". However as the incident shock continues up the hood of the truck (to which there is a slight incline), a different decay rate is sensed by the transducer at position 1. This decay rate is labeled 1 in Figure 3a. Subsequently, the incident shock hits wall b and reflects with a shock traveling toward position 1. This reflection clearly shows upon the density contour plot of Figure 4c (labeled R2). R2 eventually sweeps past gage position 1 and reflects from the floor resulting in a double peak at approximately .5 ms in Figure 3a. This is also seen in Figure 4e-f (labeled R3). Rarefactions from corner a (primarily) in Figure 3a eventually drop the pressure level to a pseudo-steady level (2 in Figure 3a).

Gage position 2 (Figure 3b) sees a pressure rise to about 40 kPa initially before it senses the reflection from wall b to a level of almost 80 kPa. This pressure is quickly reduced by the rarefaction wave generated at corner a by wave R2 (Figure 4c) as it spills over against the main flow. As it rebounds off the forward part of the floor it creates a small jump (1 in Figure 3b). Finally, R3 generates rarefaction waves at the upper corner of wall b and at corner a which combine to form decay 2 in Figure 3b. Similar waves exist in most plots.

IV. CONCLUSIONS

When comparing computed and experimental pressure-time data the general trend is very encouraging. There are tendencies to show that inclusion of viscosity will improve the computations. The steady-state values of pressures agree well with computations in all of Figure 3 except Figures 3b-c. In Figure 3b the final level is underpredicted and in Figure 3c it is overpredicted. One possible explanation is the viscous vortex set-up between the hood and the front face of the shelter, b. The two locations (2 and 4) probably don't adequately model the slow rotation in that corner. This problem appears to be very similar to the classic driven cavity problem. Pressure gradients normal to the surface are not adequately accounted for.

The computed isopycnics need further development. Shocks, in general, are captured reasonably well and contact surfaces are not. Adequate grid resolution and/or an adaptive gridding scheme should improve our results. Both avenues are being persued.

REFERENCES

1. R. W. MacCormack, "The Effect of Viscosity in Hypervelocity Impact Cratering," AIAA Paper 69-354, Cincinnati, Ohio, 1969.

2. G. Bulmash, "Shock Tube Study of a Two-Dimensional Generic Truck/Shelter Model," BRL Report in publication.

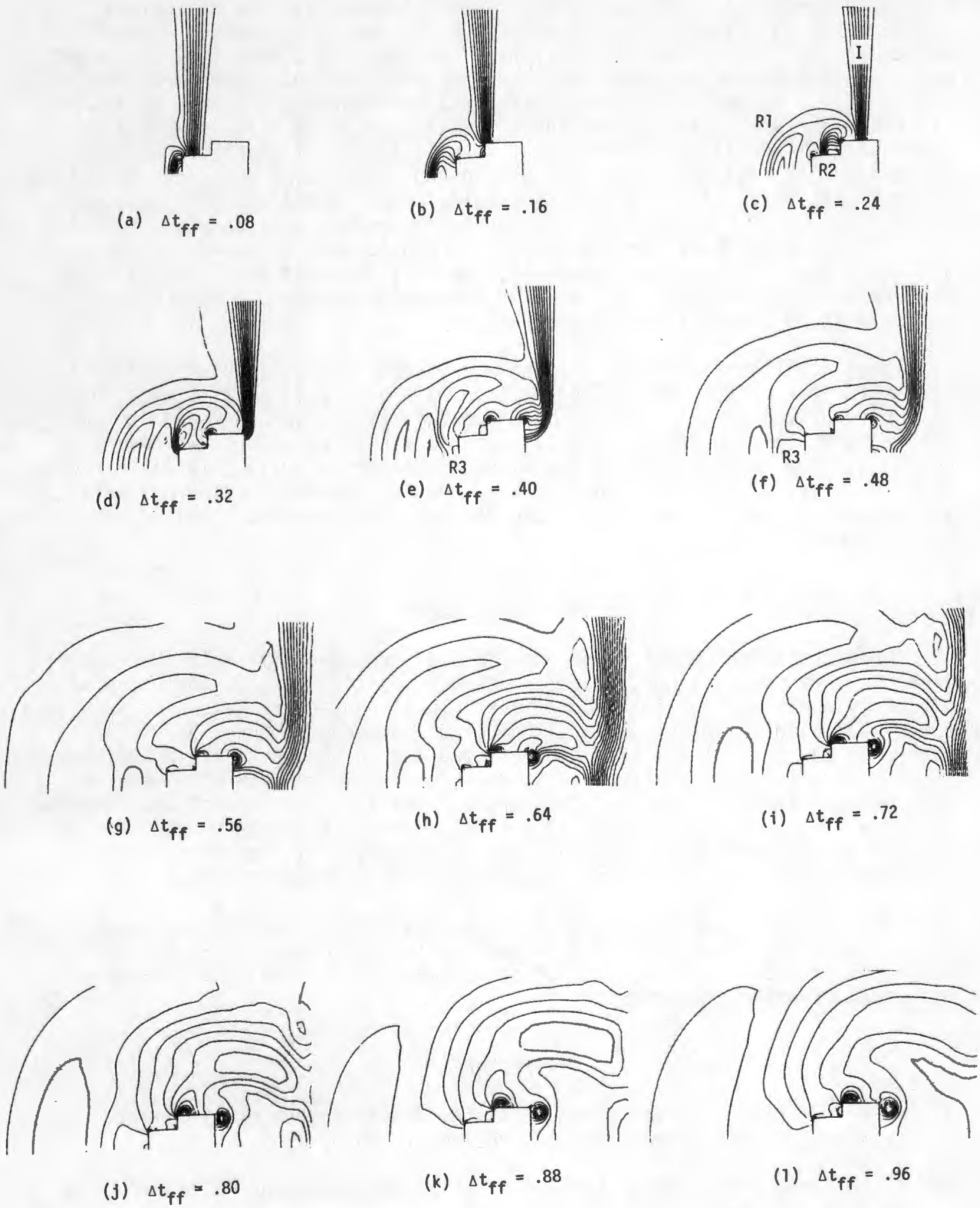

Figure 4. Computed density contours for shock wave/truck interaction. (Times after contacting front face in ms)